Int. J. Electrochem. Sci., 7 **(2012)** 2796 - 2810

International Journal of
ELECTROCHEMICAL
SCIENCE
www.electrochemsci.org

A comparative Study on the Corrosion of Monel-400 in Aerated and Deaerated Arabian Gulf Water and 3.5% Sodium Chloride Solutions

El-Sayed M. Sherif[1,*], *A. A. Almajid*[1, 2], *A. K. Bairamov*[3], *Eissa Al-Zahrani*[3]

[1] Center of Excellence for Research in Engineering Materials (CEREM), College of Engineering, King Saud University, P. O. Box 800, Al-Riyadh 11421, Saudi Arabia
[2] Department of Mechanical Engineering, College of Engineering, King Saud University, P.O. Box 800, Al-Riyadh 11421, Saudi Arabia
[3] Materials and Corrosion Section, Saudi Basic Industries Corporation (SABIC), SABIC Technology Center, P.O. Box 11669, Jubail 31961, Saudi Arabia
[*]E-mail: esherif@ksu.edu.sa

Received: 7 February 2012 / *Accepted:* 9 March 2012 / *Published:* 1 April 2012

Nickel–copper alloys are widely used as corrosion resistant materials in marine engineering. The corrosion rates of these alloys decrease sharply with increasing nickel content in the alloy. In this study, the corrosion of Monel-400 (70%Ni/30%Cu) in naturally aerated and deaerated Arabian Gulf water (AGW) and 3.5% NaCl solutions was reported. The work has been carried out using cyclic potentiodynamic polarization, chronoamperometric current-time, open-circuit potential, and electrochemical impedance spectroscopy measurements along with scanning electron microscope (SEM) and energy dispersive X-Ray analyzer (EDX) investigations. Polarization data showed that AGW is more corrosive than 3.5% NaCl towards Monel and the deaeration process decreased the corrosion of Monel in both media. Chronoamperometric curves confirmed the results obtained by polarization measurements that the uniform and pitting corrosion of Monel-400 were reduced in the deaerated AGW and 3.5% NaCl solutions. Impedance spectra revealed that the surface and polarization resistances recorded higher values in deaerated solutions. SEM/EDX investigations indicated that the corrosion of Monel-400 proceeds by the selective electrodissolution of nickel, which allows copper enrichment on the surface of the alloy.

Keywords: Arabian Gulf water; corrosion; deaeration; electrochemical measurements; Monel-400; sodium chloride solutions

1. INTRODUCTION

On account of its generally good durability in natural seawater, Monel-400 is extensively utilized in the desalination technology industry and in other marine engineering fields [1,2]. This is

because Monel-400 contains about 60-70 percent nickel, 20-29 percent copper and small amounts of iron, manganese, silicon and carbon. Monel-400 exhibits characteristics like good corrosion resistance, good weldability and high strength. Therefore, the alloy has been used extensively in many applications such as chemical processing equipment, gasoline and fresh water tanks, crude petroleum stills, valves and pumps, propeller shafts, marine fixtures and fasteners, electrical and electronic components, deaerating heaters, process vessels and piping, boiler feed water heaters and other heat exchangers, and etc [1-8]. A low corrosion rate in rapidly flowing brackish or seawater combined with excellent resistance to stress-corrosion cracking in most freshwaters, and its resistance to a variety of corrosive conditions led to its wide use in marine applications (valves and pumps that are either submerged in sea water or frequently exposed to it), oil, and chemical processing industries including non-oxidizing chloride solutions [6,9-12].

The corrosion of a series of Cu-Ni alloys in natural sea water and in chloride solutions under different conditions has been reported [3, 13–20]. Contradictory results have been obtained; some authors [13] have claimed that selective electrodissolution of nickel is predominant; while others [17] has found that copper dissolution depending on the composition of the alloy. These studies also found that the corrosion rate of the Cu-Ni alloys decreases sharply with increasing nickel content in the alloy. Although Monel-400 contains about 70% Ni and is known for its ability to stand up to tough corrosive elements, its pitting corrosion occurs when it is exposed to stagnant salt water such as seawater [8].

Seawater is a complex mixture of inorganic salts, dissolved gases, suspended solids, organic matter and organisms [18]. Arabic Gulf water (AGW) has inorganic salts that include Na^+, Mg^{2+}, K^+, Ca^{2+}, and Sr^{2+} as well as very high concentrations of chloride (24090 mg/L), and sulfate (3384 mg/L) ions. AGW also has HCO_3^-, Br-, and F^-, with total dissolved solids (TDS) of 43800 mg/L [18]. The presence of such high TDS concentration represents a very corrosive medium. Oxygen content also has a marked effect on corrosivity of seawater, and where this is reduced, as in desalination and oil-well injection systems, the seawater is much less corrosive to most materials.

The aim of the current work was to compare the anodic dissolution of Monel-400 in the aerated and deaerated Arabian Gulf water and 3.5% NaCl solutions. The study has been carried out using open-circuit potential, cyclic potentiodynamic polarization, potentiostatic current-time and electrochemical impedance spectroscopy measurements and complimented by scanning electron microscope and energy dispersive X-ray analyzer investigations.

2. EXPERIMENTAL PROCEDURE

The natural sea water (AGW) was obtained directly from the Arabian Gulf at the eastern region (Jubail, Dammam, Saudi Arabia), and was used as received. A 3.5% sodium chloride solution was prepared from the as received 99.0% NaCl, Merck. An electrochemical cell with a three-electrode configuration was used for electrochemical measurements. Monel-400 rod and sheet (were purchased from Magellan Metals, USA, with the following chemical composition, Ni–63.0% min, Cu–"28-34%" max, Fe–2.5% max, Mn–2.0%, Si–0.5% max, C–0.3% max, and S–0.024%) were used in this study.

The Monel rod was used as a working electrode. A platinum foil and a Metrohm Ag/AgCl electrode (in 3 M KCl) were used as counter and reference electrodes, respectively.

The Monel-400 rods for electrochemical measurements were grinded successively with metallographic emery paper of increasing fineness of up to 800 grits, and then polished with 1, 0.5 and 0.3μm alumina slurries (Buehler). The electrodes were then washed with doubly distilled water, degreased with acetone, washed using doubly distilled water again and finally dried with tissue paper. The diameter of the working electrode was 1.2 cm with a total exposed area of 1.13 cm^2. Electrochemical experiments were performed by using an Autolab potentiostat (PGSTAT20 computer controlled) operated by the general purpose electrochemical software (GPES) version 4.9. The cyclic potentiodynamic polarization (CPP) curves were recorded by scanning the potential in the forward direction from -800 to +800 mV then backward from +800 to -800 mV against Ag/AgCl again at the same scan rate, 3.0 mV/s. Chronoamperometric potentiostatic current-time (CT) experiments were carried out by stepping the potential of the Monel-400 electrode at +100 mV versus Ag/AgCl for 60 min. For the PPC and CT experiments, the curves were recorded after the electrode immersion in AGW and 3.5% NaCl solutions for 60 min before measurements. Electrochemical impedance spectroscopy (EIS) tests were performed after 60 min of the electrode immersion at corrosion potentials (E_{Corr}) over a frequency range of 100 kHz – 10 mHz, with an ac wave of ± 5 mV peak-to-peak overlaid on a dc bias potential, and the impedance data were collected using Powersine software at a rate of 10 points per decade change in frequency.

For experiments in deaerated media, the Monel-400 electrode was immersed after the solution was purged with pure nitrogen for 60 min and the cell was kept purged above the solution until the end of the experiment. This was followed for all deaerated experiments in order to avoid oxygen penetration into the AGW and 3.5% NaCl solutions during the measurements.

The SEM images were obtained by using a JEOL model JSM-6610LV (Japanese made) scanning electron microscope with an energy dispersive X-ray analyzer attached for acquiring the EDX analysis.

3. RESULTS AND DISCUSSION

3.1. Cyclic potentiodynamic polarization (CPP) measurements

Fig. 1 shows the cyclic potentiodynamic polarization (CPP) curves for Monel-400 that was immersed for 1 h in naturally aerated solutions of (a) AGW and (b) 3.5% NaCl solutions. CPP experiments were carried out to report the corrosion parameters and to compare between the effect of AGW and NaCl solutions on the corrosion Monel-400. Parameters such as corrosion potential (E_{Corr}), Corrosion current (j_{Corr}), pitting potential (E_{Pit}), pitting current (j_{Pit}), polarization resistance (R_P), and corrosion rate (K_{Corr}) were determined and calculated from the polarization curves according to our previous work [21-34].

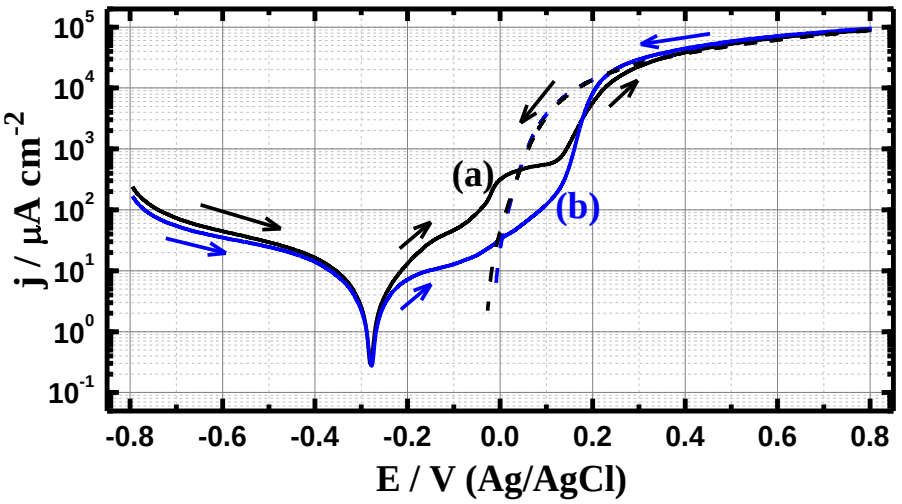

Figure 1. Cyclic potentiodynamic polarization curves for Monel-400 that was immersed for 1 h in naturally aerated solutions of **(a)** AGW and **(b)** 3.5% NaCl solutions.

It is clearly seen from Fig. 1 that an active dissolution of the alloy occurred with increasing potential in the anodic side. It has been reported [15, 19] that the anodic reaction of Monel-400 is the selective dissolution of nickel, particularly at high potential values. Increasing the applied potential in the anodic branch leads to the appearance of a peak at which the current started to decrease due to either the formation of a passive oxide film [35, 36] or the accumulation of corrosion products on the electrode surface. The current then increased suddenly as a result of the breakdown of the passive film formed on alloy surface in seawater leading to the occurrence of pitting corrosion [37, 38]. Further increasing the positive potential increases the anodic current. According to Gouda et al. [8], the current increases due to the dissolution of Monel through the agglomeration of chloride ions inside the pits leading to pit growth. It is also seen that AGW (Fig. 1a) is more aggressive than 3.5% NaCl (Fig. 1b) towards the anodic dissolution of Monel as the current recorded higher values for AGW than NaCl.

CPP curves for Monel-400 that was immersed for 1 h in (1) naturally aerated and (2) deaerated solutions of (a) AGW and (b) NaCl respectively are shown in Fig. 2. It is clearly seen from Fig. 2a that the cathodic current of Monel is high in case of naturally aerated AGW than the deaerated one. This can be attributed to the kind of the cathodic reaction of Monel-400, where it is the oxygen reduction in aerated near neutral solutions as follows,

$$2H_2O + O_2 + 4e^- = 4OH^- \quad (1)$$

While in the deaerated solutions, the cathodic reaction is mainly the reduction of water to produce hydroxide ions [39-41] as follows,

$$2H_2O + 2e^- = H_2 + 2OH^- \quad (2)$$

It is well know that the oxygen reduction is stronger than the water reduction as cathodic reaction, which explains the higher current values for Monel in aerated AGW.

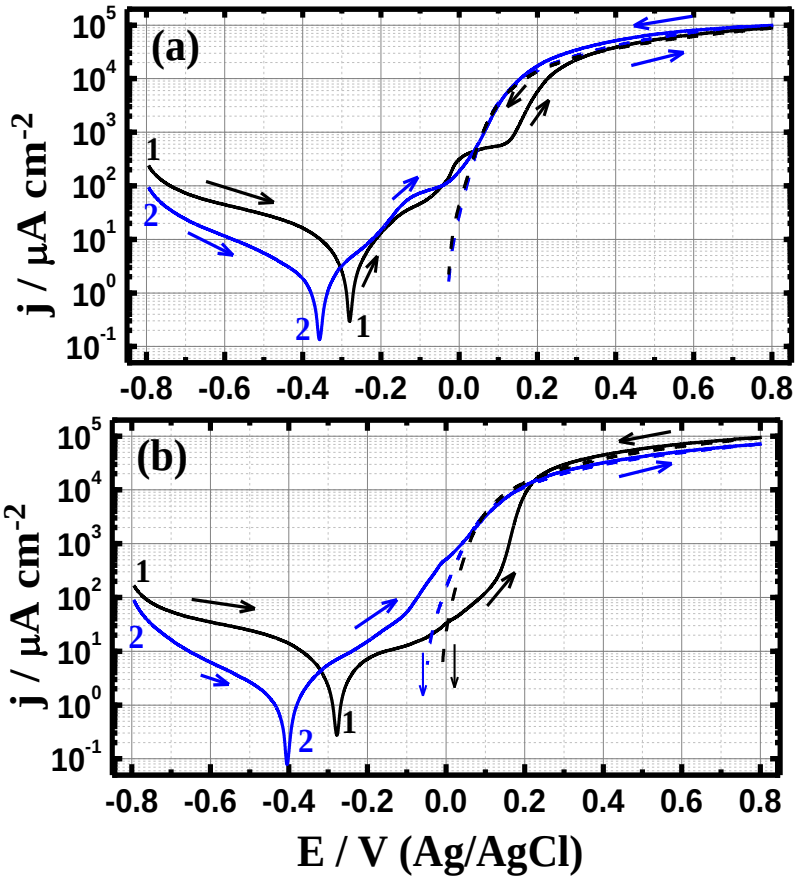

Figure 2. Cyclic potentiodynamic polarization curves for Monel-400 that was immersed for 1 h in (1) naturally aerated and (2) deaerated solutions of **(a)** AGW and **(b)** 3.5% NaCl, respectively.

Table 1. Corrosion parameters obtained from cyclic polarization curves for the Monel-400 alloy in the AGW and 3.5% NaCl solutions.

Solution	Parameter						
	β_c/mV dec^{-1}	E_{Corr}/ mV	j_{Corr}/ μA cm^{-2}	β_a/mV dec^{-1}	E_{Pit}/ mV	R_p/ Ω cm^2	K_{Corr}/ mmy^{-1}
Aerated AGW	220	-257	5.8	130	120	6.12	0.0770
De-aerated AGW	230	-353	1.5	135	60	24.66	0.0200
Aerated NaCl	180	-260	4.0	185	140	9.92	0.0531
De-aerated NaCl	200	-412	1.3	190	30	32.59	0.0173

Purging the nitrogen into the solution, Fig. 2a, curve 2, decreased the values of corrosion current density (j_{Corr}), shifted the corrosion potential (E_{Corr}) to a more negative value and decreased the anodic current. The values j_{Corr} and E_{Corr} in addition to the values of cathodic Tafel slope (β_c), anodic Tafel slope (β_a), corrosion resistance (R_P), and corrosion rate (K_{Corr}) that were obtained for the

polarization curves shown in Fig. 2 are listed in Table 1. Fig. 2a and Table 2 prove that the deaeration process also increased the value of R_P and decreased the value of K_{Corr}. This indicates that the anodic dissolution of Monel-400 in AGW decreases in absence of oxygen.

3.2. Chronoamperometric current-time (CT) measurements

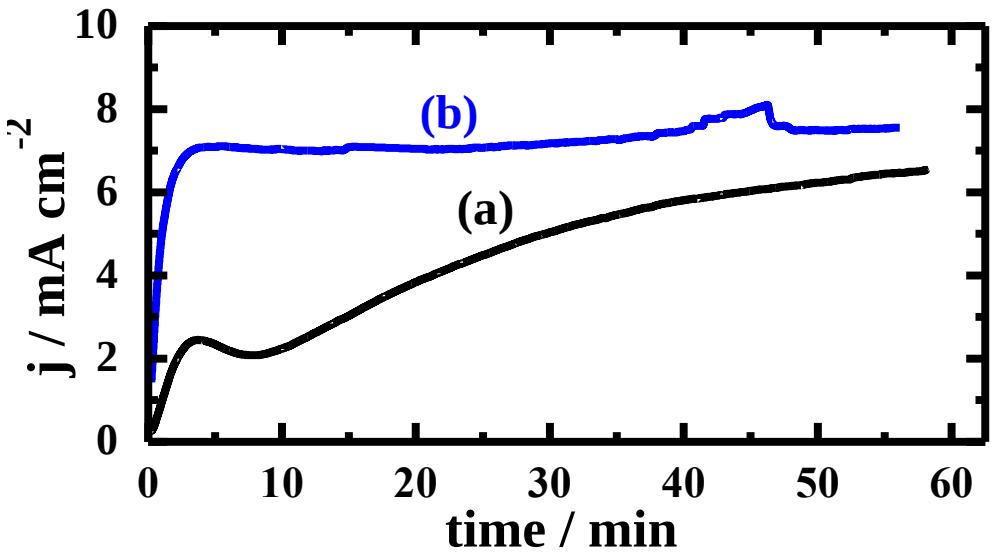

Figure 3. Chronoamperometric curves obtained at 100 mV vs. Ag/AgCl for the Monel-400 electrode that was immersed for 1 h in naturally aerated solutions of **(a)** AGW and **(b)** 3.5% NaCl.

In order to shed more light on the effect of deaeration on both uniform and pitting corrosion of Monel-400 in stagnant AGW and NaCl solutions at a more positive potential value, chronoamperometric experiments were carried out at 100 mV vs. Ag/AgCl. The variations of current values with time at 100 mV vs. Ag/AgCl for Monel-400 after 1 h immersion in freely aerated (a) AGW and (b) 3.5% NaCl solutions, respectively are shown in Fig. 3. It is clearly seen that the current for Monel-400 in AGW, Fig. 3, curve a, recorded very low values in the first few moments of the measurement. This might be due to the accumulation of corrosion products and/or scales form sea water on the Monel surface, which in turn partially block the surface form being attacked by the surrounding environment. Increasing the time increased the current values as a result of the aggressive ions attack present in the sea water on the flawed areas of the Monel surface leading to the occurrence of pitting corrosion. For Monel-400 in 3.5% NaCl solutions, Fig. 3, curve b, the current showed a rapid increase in its initial values in the first 200 seconds might be due to the dissolution of a peroxide film was formed on the electrode surface in air before its immersion in the electrolyte. The current then decreased and stayed almost constant till the end of the experiment. Comparing the effect of AGW and 3.5% NaCl, one can conclude that Monel-400 suffers high pitting corrosion in AGW, while its shows higher uniform attack in 3.5% NaCl solutions.

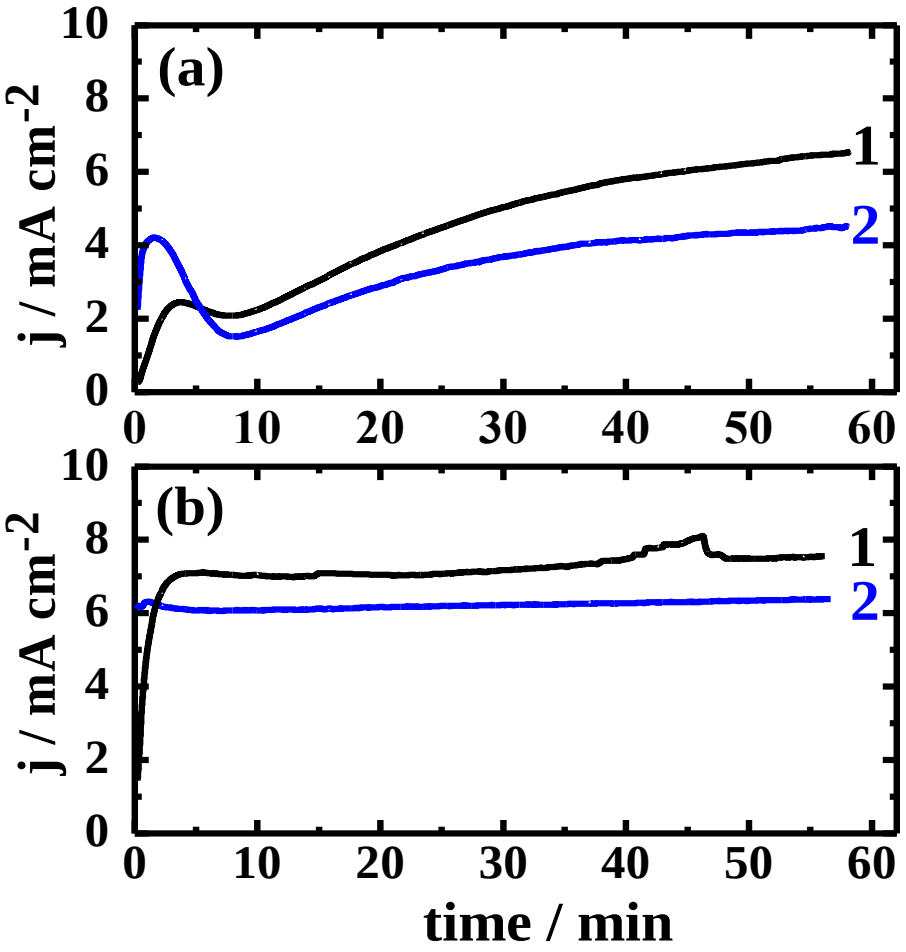

Figure 4. Chronoamperometric curves obtained at 100 mV vs. Ag/AgCl for the Monel-400 electrode that was immersed for 1 h in (1) freely aerated and (2) de-aerated solutions of **(a)** AGW and **(b)** 3.5% NaCl.

Chronoamperometric curves obtained at 100 mV vs. Ag/AgCl for the Monel electrode that was immersed for 1 h in (1) freely aerated and (2) deaerated solutions of (a) AGW and (b) NaCl are shown in Fig. 4, respectively. The variation of current in deaerated AGW, Fig. 4, curve 2, showed higher values compared to the freely aerated one, because the absence of oxygen by deaeration did not allow the Monel surface to develop corrosion products, which partially protect the alloy and decrease the uniform corrosion. Increasing the time led to decrease the absolute current values due to the decrease of uniform attack on the Monel surface. In 3.5% NaCl solutions, the deaeration increased the initial current values and for the rest of the experiment the absolute current was lower than that recorded for the alloy in the aerated solutions. From the chronoamperometric measurements, it can be concluded that the deaeration process decreases both the uniform and pitting corrosion of the Monel. This can be explained on the basis that the cathodic reaction of Monel in the deaerated solutions (Eq. 2) is the water reduction, which is weaker than the oxygen reduction reaction in the freely aerated solutions (Eq. 1). The cathodic reaction consumes the electrons that are produced in the dissolution process of the anodic reaction, which is why the weaker the cathodic reaction the lower the dissolution of Monel.

The CT data thus confirm the results obtained from the polarization measurements that the deaeration decreases both uniform and pitting corrosion of Monel-400 in AGW and 3.5% NaCl solutions.

3.3. Open-circuit potential (OCP) measurements

The change of the corrosion potential (OCP) within 60 h of the Monel-400 electrode immersion in aerated stagnant solutions of AGW (a) and 3.5% NaCl (b), respectively is shown in Fig. 5. The OCP of Monel-400, Fig. 5a, showed a slight decrease toward the negative values in the first 5 h, most probably due to the dissolution of Monel. This slight negative potential shift slowed down with increasing the immersion time up to the first 45 h, which might be due to the formation of corrosion products and/or scales on the surface. These partially protected the alloy surface and led to decreasing the potential in the positive direction till the end of the test. This very slight positive shift in the OCP values decreased the corrosion rate by decreasing the uniform attack of the alloy with time.

The OCP of Monel in 3.5% NaCl solution, Fig. 5b, recorded circa 30 mV less negative potential value than that obtained for AGW at the first moment of electrode immersion. The potential then exhibited a rapid shift towards the negative direction in the first 25 min has a result of the dissolution of Monel-400. Increasing the time further led to a very slight shift in the OCP values and up to the end of the run, which might be due to the formation of corrosion products on the alloy surface. The formation of such corrosion products partially protected the alloy surface and decreased its uniform corrosion with time. It is worth mentioning that AGW is more corrosive than 3.5% NaCl at the early immersion time, the first 16 h, after which Monel suffers more attack by NaCl than AGW. This perhaps due to the fact that Monel not only develops corrosion products in AGW but also scales, which in turn decrease its uniform corrosion with time. This is in good agreement with the conclusion obtained from the polarization and chronoamperometric measurements.

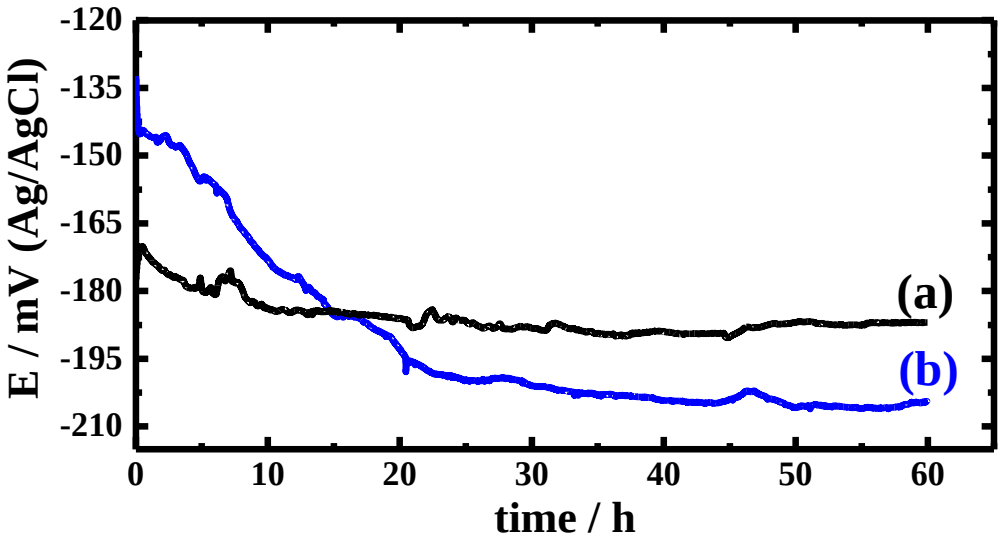

Figure 5. Variations of the open-circuit potential versus time for Monel-400 in **(a)** Arabian Gulf water and **(b)** 3.5% NaCl solutions

3.4. Scanning electron microscope (SEM) and energy dispersive X-ray (EDX) investigations

Figure 6 shows the SEM micrographs (a) and the corresponding EDX profile analysis (b), respectively for Monel-400 after its immersion in AGW for 160 days. One can see from Fig. 6a for the Monel in seawater that the surface shows a flat area covered with some corrosion products in addition to a wide pit, which is also covered with corrosion products. This proves that Monel suffers pitting corrosion when exposed to stagnant AGW for long immersion time. The atomic percentages of the elements found in the selected area of image (a) by the EDX profile shown in Fig 6b, were 41.80% C, 35.28% O, 12.75% Ni, 6.33% Cu, 2.86% Cl, 0.49% Fe, 0.29% S, and 0.19% Mn. The low contents of Ni and Cu and the high percentages of C and O suggest that the alloy surface is covered with corrosion products that have different compounds, complexes and oxides.

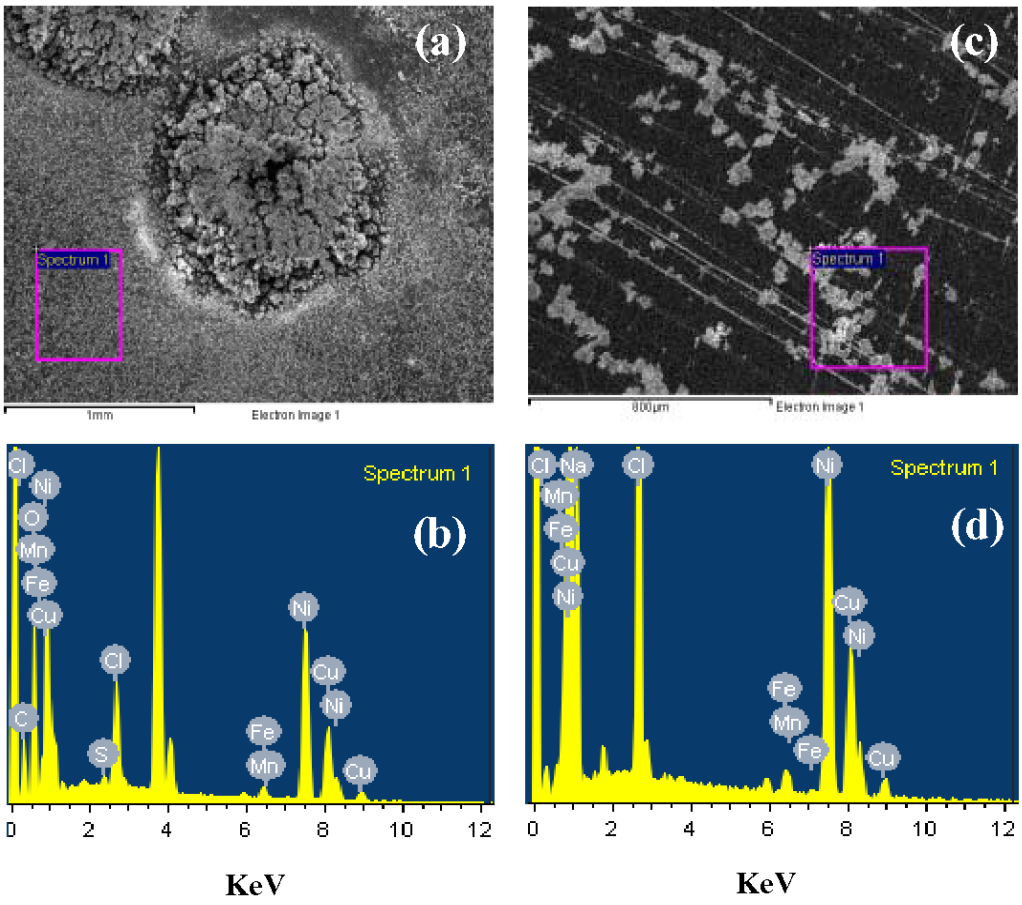

Figure 6. SEM micrograph (a) and the corresponding EDX profile analysis (b) for Monel-400 after its immersion in AGW for 160 days, while (c) and (d) are the SEM and EDX for Monel-400 in 3.5% NaCl solutions at the same condition, respectively.

The presence of chloride, sulphur and iron besides carbon also suggest that the surface is having scales deposited from the seawater. It is worthy to mention also that the elements found inside the pit [2] were very high copper content and very low Ni content, which confirms the selective

dissolution of Ni with copper enrichment. It was also found that [2] the presence of oxygen inside the pit was poor compared to its percentages on the surface and around the pit. This specifies that aggressive ions such as Cl^- displace the oxygen at its weakest bond with metal on the alloy surface and initiate pitting corrosion. The presence of Cl^- at such content raises the potential difference across the passive film, thereby enhancing the rate of nickel ions diffusion from the nickel-film interface to the film-solution interface, forming cation vacancies at the Monel-film interface [8].On the other hand and in order to see the surface morphology and to identify the composition of the species formed on the Monel-400 surface after its immersion in 3.5% NaCl for 160 days, SEM/EDX investigations were carried out as shown in Fig. 6c and Fig. 6d, respectively. It is clearly seen from the SEM image presented in Fig. 6c that there are black and white areas with no pits observed on the Monel surface. The atomic percentage of the elements found in the selected area shown in Fig. 6c and displayed in the EDX profile presented in Fig. 6d, were 43.42% Na, 13.26% Cl, 1.05% Fe, 0.62% Mn, 28.25% Ni, and 13.40% Cu. This indicates that the surface in this area is containing the main alloying elements having almost less than half of their actual percentages, in addition to high content of NaCl salt. This may indicate also that the white colour presented on the surface is probably for NaCl salt, while the black areas contain the main component of the alloy. SEM/EDX investigations thus confirm that AGW is more corrosive towards Monel-400 compared to 3.5% NaCl, which also confirm the data obtained by polarization and chronoamperometry.

3.5. Electrochemical impedance spectroscopy (EIS) investigations

The Nyquist plots (a), Bode (b), and phase angle (c) for Monel-400 at an OCP after its immersion for 1 h in (1) freely aerated and (2) de-aerated solutions of AGW, respectively are shown in Fig. 7. The Nyquist (a), Bode (b) and phase angle (c) plots for Monel-400 in (1) freely aerated and (2) de-aerated solutions of 3.5% NaCl at the same conditions are also shown in Fig. 8. The impedance spectra of the Nyquist plots shown in Fig. 7a and Fig. 8a were analysed by fitting to the equivalent circuit model shown in Fig. 9. The parameters obtained from the equivalent circuit are listed in Table 2. Here, R_S represents the solution resistance between the Monel and the counter (platinum) electrode, Q the constant phase elements (*CPEs*) and contain two parameters; a pseudo capacitance and an exponent, the R_{P1} accounts for the resistance of a film layer formed on the Monel surface, C_{dl} is the double layer capacitance, and R_{P2} accounts for the charge transfer resistance at the alloy surface, i.e. the polarization resistance [42-44].

It is clearly seen from Fig. 7, Fig. 8, and Table 4 that the values of R_S, R_{P1} and R_{P2} recorded for Monel in NaCl are greater than that for AGW solutions and these values increased when the solutions were deaerated. The reason for the high values of these resistances in NaCl is because the AGW solution is more aggressive towards Monel than 3.5% NaCl. While, their increase in the deaerated solutions is attributed to the lower cathodic reaction compared to the aerated solutions and thus decrease the attack on the Monel surface. This in turn decreases the corrosion rate and could lead to the decrease in j_{Corr} and K_{Corr} and also the increase in R_P values we have seen in polarization data (Fig. 1, Fig. 2, and Table 1) under the same conditions.

The semicircles at high frequencies in Fig. 7a and Fig. 8a are generally associated with the relaxation of electrical double layer capacitors and the diameters of the high frequency semicircles can be considered as the charge transfer resistance ($R_P = R_{P2} + R_{P2}$) [45-48]. It is also observed that increasing the deaeration process leads to increasing the impedance of the interface (Fig. 7b and Fig. 8b) and the maximum phase angle (Fig. 7c and Fig. 8c). In general, the polarization resistance measured by EIS is a measure of the uniform corrosion rate as opposed to tendency towards localized corrosion. The EIS data is thus in good agreement with polarization measurements that deaeration of AGW and 3.5% NaCl solutions highly decrease the corrosion of Monel in both media.

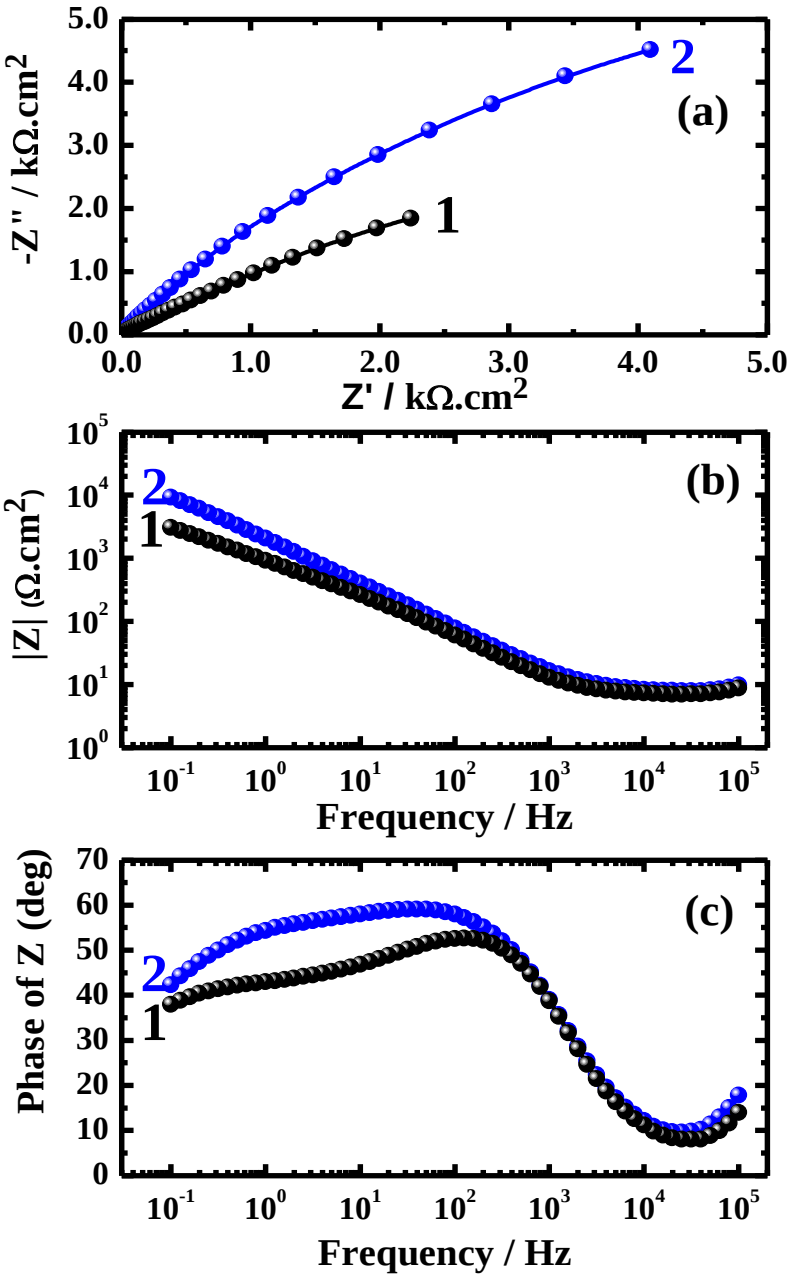

Figure 7. Nyquist **(a)**, Bode **(b)** and phase angle **(c)** plots for Monel-400 at an OCP after its immersion for 1 h in (1) freely aerated and (2) de-aerated solutions of AGW.

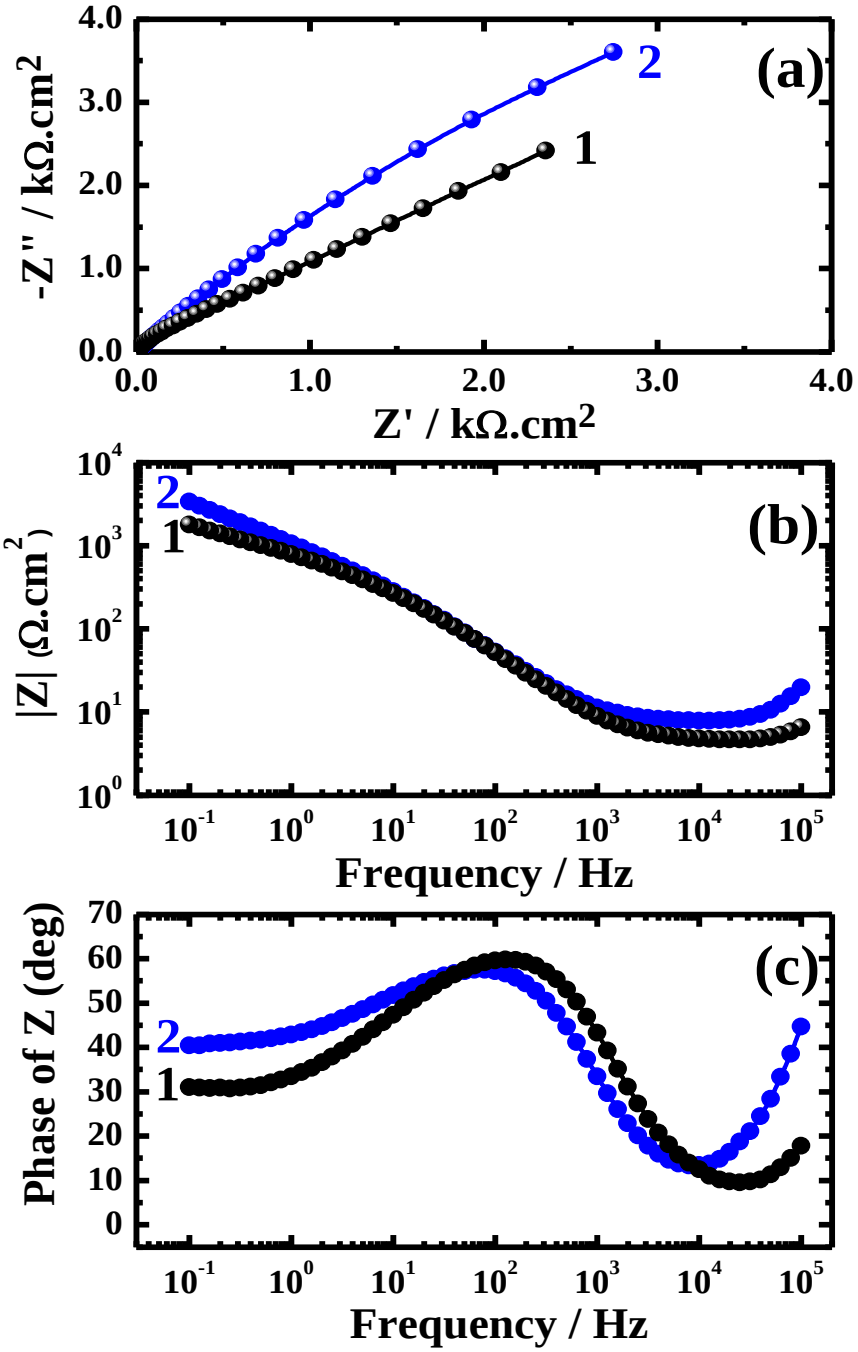

Figure 8. Nyquist **(a)**, Bode **(b)** and phase angle **(c)** plots for Monel-400 at an OCP after its immersion for 1 h in (1) freely aerated and (2) de-aerated solutions of 3.5% NaCl.

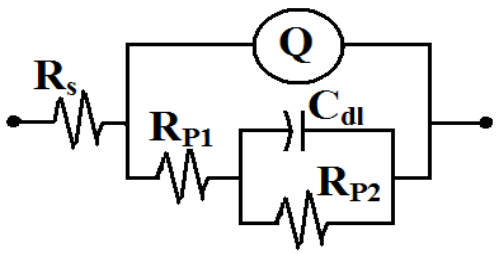

Figure 9. The equivalent circuit used to fit the experimental data presented in Fig. 7a and Fig. 8a. See text for symbols used in the circuit.

Table 2. EIS parameters obtained by fitting the Nyquist plots with the equivalent circuit for the Monel-400 in AGW and 3.5% NaCl solutions.

Medium	Parameter					
	R_s / Ωcm^2	Q (CPEs)		R_{p1} / $K\Omega cm^2$	Cdl / μFcm^{-2}	R_{p2} / $K\Omega cm^2$
		Y_Q / μFcm^{-2}	n			
Aerated AGW	4.96	11.95	0.70	0.63	23.47	2.082
De-aerated AGW	8.50	1.81	0.80	1.82	0.116	3.88
Aerated NaCl	5.15	9.57	0.50	0.71	8.26	2.45
De-aerated NaCl	6.79	2.77	0.70	1.47	0.216	3.58

4. CONCLUSIONS

The corrosion of Monel-400 in naturally aerated and deaerated solutions of Arabian Gulf water and 3.5% NaCl has been studied at room temperature by using different electrochemical and spectroscopic test methods. The outcome results can be summarized as follows:

1. Polarization measurements indicated that pitting corrosion occurred for Monel in both AGW and NaCl solutions due to the attack of corrosive species such as Cl^- to the weakest oxygen-alloy bond and that a selective dissolution of Ni leads to the propagation of the formed pits.
2. Polarization tests also stated that AGW is more corrosive than 3.5% NaCl towards and the deaeration process decreased the corrosion of Monel in both media.
3. Current-time curves recorded for the Monel at 100 mV revealed that deaerating the AGW and 3.5% NaCl solutions decreases both pitting and general corrosion.
4. Electrochemical impedance spectroscopy confirmed the polarization and current-time, where the surface and polarization resistances recorded higher values in NaCl as well as in deaerated solutions, which indicates that AGW is more corrosive than NaCl and deaerated solutions are much less aggressive.
5. SEM images and EDX profiles indicated that pitting corrosion occurs faster for Monel in AGW and the surface develops a mixture of oxides, chlorides, and/or oxy-chloride complexes with a selective dissolution of Ni.
6. The results collectively are internally consistent with each other, showing that AGW is more aggressive than 3.5% NaCl solution and the deaeration process decreases the severity of both solutions.

ACKNOWLEDGEMENT
The authors are grateful to the Center of Excellence for Research in Engineering Materials (CEREM) for the financial support.

References

1. T. Hodgkiess, G. Vassiliou, *Desalination*, 183 (2005) 235.
2. El-Sayed M. Sherif, A.A. Almajid, A.K. Bairamov, E. Al-Zahrani, *Int. J. Electrochem. Sci.*, 6 (2011) 5430.

3. J.A. Ali, *Corros. Sci.,* 36 (1994) 773.
4. J.A. Ali, J.R. Ambrose, *Corros. Sci.,* 32 (1991) 799.
5. C.J. Semino, P. Pedeferri, G.T. Burstein, T.P. Hoar, *Corros. Sci.,* 19 (1979) 1069.
6. S.K. Ghosh, G.K. Dey, R.O. Dusane, A.K. Grover, *J. Alloy. Compd.,* 426 (2006) 235.
7. S. Hettiarachchi, T.P. Hoar, *Corros. Sci.,* 19 (1979) 1059.
8. V.K. Gouda, I.Z. Selim, A.A. Khedr, A.M. Fathi, *J. Mater. Sci. Technol.,* 15 (1999) 208.
9. H. Hebert Ulig, *Corrosion and Corrosion Control*, John Wiley & Sons Inc. 1963.
10. J. Crousier, A.M. Beccaria, *Werks. Korros.*, 41 (1990) 185.
11. Colin R. Gagg, Peter R. Lewis, *Engineering Failure Analysis*, 15 (2008) 505.
12. A.U. Malik, S. Ahmad, I. Andijani, S. Al-Fouzan, *Desalination*, 123 (1999) 205.
13. H.P. Lee, Ken Nobe, *J. Electrochem. Soc.,* 131 (1984) 1236.
14. M.E. Walton, P.A. Brook, *Corros. Sci.,* 17 (1977) 317.
15. R.G. Blundy, M.J. Proyor, *Corros. Sci.,* 12 (1972) 65.
16. M. Metikoš-Huković, R. Babić, I. Škugor, Z. Grubač, *Corros. Sci.,* 53 (2011) 347.
17. Saleh A. Al-Fozan, Anees U. Malik, *Desalination,* 228 (2008) 61.
18. A.M. Shams El Din, M.E. El Dahshan, A.M. Taj El Din, *Desalination,* 130 (2000) 89.
19. J.T. Francis, N.S. McIntyre, R.D. Davidson, S. Ramamurthy, A.M. Brennenstühl, A. McBride, A. Roberts, *Surf. Interface Anal.,* 33 (2002) 29.
20. K. Habib, A. Fakhral-Deen, *Desalination*, 139 (2001) 249.
21. El-Sayed M. Sherif, A. A. Almajid, *Int. J. Electrochem. Sci.,* 6 (2011) 2131.
22. El-Sayed M. Sherif, *Int. J. Electrochem. Sci.,* 6 (2011) 1479.
23. El-Sayed M. Sherif, R. M. Erasmus, J. D. Comins, *Electrochim. Acta,* 55 (2010) 3657.
24. El-Sayed M. Sherif, *Int. J. Electrochem. Sci.,* 6 (2011) 3077.
25. El-Sayed M. Sherif, *Mater. Chem. Phys.,* 129 (2011) 961.
26. El-Sayed M. Sherif, *J. Mater. Eng. Perform.,* 19 (2010) 873.
27. El-Sayed M. Sherif, A.A. Almajid, *J. Appl. Electrochem.,* 40 (2010) 1555.
28. El-Sayed M. Sherif, A.A. Almajid, F.H. Latif, H. Junaedi, *Int. J. Electrochem. Sci.,* 6 (2011) 1085.
29. El-Sayed M. Sherif, *Int. J. Electrochem. Sci.,* 6 (2011) 2284.
30. El-Sayed M. Sherif, A.H. Ahmed, *Synthesis and Reactivity in Inorganic, Metal-Organic and Nano-Metal Chemistry,* 40 (2010) 365.
31. El-Sayed M. Sherif, J.H. Potgieter, J.D. Comins, L. Cornish, P.A. Olubambi, C.N. Machio, *J. Appl. Electrochem.,* 39 (2009) 83.
32. El-Sayed M. Sherif, J.H. Potgieter, J.D. Comins, L. Cornish, P.A. Olubambi, C.N. Machio, *Corros. Sci.,* 51 (2009) 1364.
33. F.H. Latief, El-Sayed M. Sherif, A.A. Almajid, H. Junaedi, *J. Anal. Appl. Pyrol.,* 92 (2011) 485.
34. El-Sayed M. Sherif, *Int. J. Electrochem. Sci.,* 6 (2011) 5372.
35. W.Z. Friend, ed., "*Corrosion of Nickel and Nickel-Based Alloys*", Houston, TX: NACE International (1980).
36. M. Stern, *J. Electrochem. Soc.,* 106 (1959) 376.
37. M.A. Streicher, *J. Electrochem. Soc.,* 103 (1956) 375.
38. W. Schwenk, *Corrosion*, 20 (1964) 129t.
39. E.M. Sherif, S.-M. Park, *J. Electrochem. Soc.,* 152 (2005) B428.
40. H. Otmacic, E. Stupnisek-Lisac, *Electrochim. Acta*, 48 (2002) 985.
41. K.A. Khalil, El-Sayed M. Sherif, A.A. Almajid, *Int. J. Electrochem. Sci.,* 6 (2011) 6184.
42. El-Sayed M. Sherif, R. M. Erasmus, J. D. Comins, *J. Appl. Electrochem.,* 39 (2009) 83.
43. R.D. Klassen and P.R. Roberge, Y. Wang, Corrosion resistance of UNS N04400 vs. electroless nickel in simulated marine service, *Corrosion, Paper No. 05232,* NACE International, Houston, Texas (2005).
44. El-Sayed M. Sherif, R. M. Erasmus, J. D. Comins, *Corros. Sci.,* 50 (2008) 3439.
45. E.M. Sherif, S.-M. Park, *Electrochim. Acta,* 51 (2006) 6556.

46. H. Ma, S. Chen, L. Niu, S. Zhao, S. Li, D. Li, *J. Appl. Electrochem.*, 32 (2002) 65.
47. El-Sayed M. Sherif, *Int. J. Electrochem. Sci.*, 7 (2012) 1482.
48. El-Sayed M. Sherif, Corrosion of Duplex Stainless Steel Alloy 2209 in Acidic and Neutral Chloride Solutions and its Passivation by Ruthenium as an Alloying Element, *Int. J. Electrochem. Sci.*, 7 (3) (2012) in press.